LANGMUIR

pubs.acs.org/Langmuir Article

Polyethylene Glycol Crowder's Effect on Enzyme Aggregation, Thermal Stability, and Residual Catalytic Activity

Xue Wang, Jeremy Bowman, Sidong Tu, Dmytro Nykypanchuk, Olga Kuksenok, and Sergiy Minko*

Cite This: *Langmuir* 2021, 37, 8474–8485 Read Online

ACCESS | Metrics & More | Article Recommendations | Supporting Information

ABSTRACT: Protein stability and performance in various natural and artificial systems incorporating many other macromolecules for therapeutic, diagnostic, sensor, and biotechnological applications attract increasing interest with the expansion of these technologies. Here we address the catalytic activity of lysozyme protein (LYZ) in the presence of a polyethylene glycol (PEG) crowder in a broad range of concentrations and temperatures in aqueous solutions of two different molecular mass PEG samples (M_w = 3350 and 10000 g/mol). The phase behavior of PEG−protein solutions is examined by using dynamic light scattering (DLS) and small-angle X-ray scattering (SAXS), while the enzyme denaturing is monitored by using an activity assay (AS) and circular dichroism (CD) spectroscopy. Molecular dynamic (MD) simulations are used to illustrate the effect of PEG concentration on protein stability at high temperatures. The results demonstrate that LYZ residual activity after 1 h incubation at 80 °C is improved from 15% up to 55% with the addition of PEG. The improvement is attributed to two underlying mechanisms. (i) Primarily, the stabilizing effect is due to the suppression of the enzyme aggregation because of the stronger PEG−protein interactions caused by the increased hydrophobicity of PEG and lysozyme at elevated temperatures. (ii) The MD simulations showed that the addition of PEG to some degree stabilizes the secondary structures of the enzyme by delaying unfolding at elevated temperatures. The more pronounced effect is observed with an increase in PEG concentration. This trend is consistent with CD and AS experimental results, where the thermal stability is strengthened with increasing of PEG concentration and molecular mass. The results show that the highest stabilizing effect is approached at the critical overlap concentration of PEG.

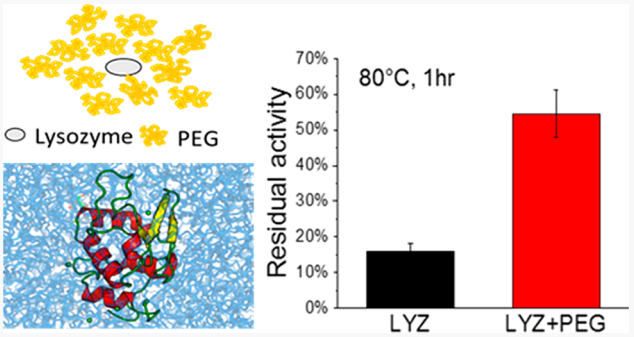

INTRODUCTION

Industrial and biomedical applications of enzymes continue to expand because of their unique catalytic efficiency and selectivity.[1−7] Many mesophilic enzymes have poor thermal stability and poor retention of their catalytic activity above 50−60 °C,[8−10] thus limiting their applications when extended use at elevated temperatures is beneficial to increase productivity and decrease bacterial contamination of the industrial processes[11] and when enzyme storage requires a low temperature. Simple and cost-efficient methods to improve enzyme stability are in high demand.

The hydrophobic effect plays a major role in stabilizing protein globules in an aqueous solution.[1213] The temperature increase, however, results in the increase of the conformational entropy upon unfolding. Hence, at high temperature the hydrophobic interactions are no longer sufficient to compensate for the loss of conformational entropy upon folding,[14] and water molecules penetrate the globule causing degradation of the secondary structures.

Numerous approaches have been proposed to address the problem of proteins' thermal stability. All the methods could be broken down into two large groups. The first group is the development of synthetic proteins with improved thermal stability through a modification of amino acid sequence to enlarge the hydrophobic effect or provide additional cross-linking.[15−17] The second group is based on binding of protein molecules with organic molecules (mainly with polymers)[18] or solid particles (often porous structures)[19−21] to reinforce the protein globule, screen penetration of water molecules, and minimize irreversible aggregation. Both of these groups of methods are essential because neither of these methods can be universally applied for different applications of proteins. Herein, we are interested in the second group of methods, specifically in the mechanism of improvement of the protein stability via interactions with polymeric additives. Protein−polymer systems are studied for two major aspects of their applications: (i) improvement of protein stability for storage, transportation, and biotechnological processes at elevated

Received: March 29, 2021
Revised: May 25, 2021
Published: July 8, 2021

https://doi.org/10.1021/acs.langmuir.1c00872
Langmuir 2021, 37, 8474−8485

temperatures and (ii) understanding of protein interactions in a complex natural or synthetic environment that includes natural or synthetic macromolecules. In the latter case, the relevant examples of the applications are in protein therapeutic drugs[22] and growth factors for cell culturing.[23]

Mechanisms of thermal denaturing of proteins in the presence of polymers have many aspects that are specific for each protein. Indeed, many commonly observed mechanisms allow for the development of general concepts for understanding polymer−protein interactions and their effect on denaturing mechanisms. In this work, we study thermal denaturation of lysozyme enzyme in the presence of polyethylene glycol (PEG) or polyethylene oxide (PEO); the same polymer is traditionally referred to PEG for molecular mass <20 kg/mol and PEO for molecular mass >20 kg/mol. Both PEG and PEO terms are used in our discussion when we refer to original publications. LYZ has been extensively investigated, which makes it quite a convenient subject for research.[24] We anticipate that many aspects of the stabilization established for the PEG−lysozyme system could be considered for other PEG−protein systems.

Hen egg-white lysozyme (LYZ) used in this study is a monomeric protein consisting of 129 amino acid residues and cross-linked by four disulfide bridges.[25] The mechanism of LYZ thermal denaturation can be depicted by the classical scheme of Lumry and Eyring:[26] $N \rightleftarrows U \rightarrow I$, where the native enzyme, N, reversibly unfolds to the denatured state, U, followed by the irreversible transition to the inactive conformation, I. The denaturing process is pH-dependent. LYZ can be irreversibly inactivated at 100 °C as a result of deamidation of asparagine residues at pH 4[27,28] and a combination of aggregation and intermolecular/intramolecular disulfide exchanges (disulfide scrambling) at neutral pH (a range of pH from 6 to 8).[29] The secondary structure of LYZ is dominated by α-helix and minor β-sheet and turn elements. With a progressive rise in temperature, the α-helix structure unfolds. These conformational changes are followed by aggregation of the enzyme and irreversible loss of activity.

The greatest LYZ thermal stability was measured at pH 5. It was found that at pH 5 LYZ demonstrated minimal changes in the secondary structure with minimal aggregation, hence with maximal stability in a temperature range from the room temperature to 70 °C.[30] The aggregation via the interaction between hydrophobic fragments of the unfolded enzyme remains irreversible upon cooling or dilution.[31,32] LYZs begin to unfold at around 50 °C and then aggregate at about 70 °C. At the latter stage, protein globules are denatured and aggregated.[33] Disulfide scrambling, which takes place at neutral to alkaline pH,[29,34] is also accompanied by aggregation.[35]

Our previous studies of LYZ−polymer conjugates demonstrated a significant improvement of the enzyme thermal stability at pH 5.2.[36,37] In these studies, LYZ was conjugated with a PEO bottlebrush constituted of the acrylate backbone with PEG side chains. The enzyme was covalently bound to the backbone of the bottlebrush between the PEG side chains. The half-life of the lysozyme−polymer conjugate at 90 °C was extended 9-fold. The possible explanation of the improved enzyme performance is the so-called "crowding effect" caused by PEG side chains in the bottlebrush structure. However, this explanation remained a hypothesis.

Notably, PEG is often used for enzyme stabilization either via conjugation with enzymes[11,38−43] or via the addition of PEG into the medium.[11,44,45] PEGylation, or covalent binding of PEG to proteins, results in a PEG−protein conjugate. PEGylation often improves the stability of the secondary structure,[11,38−43] including mechanical reinforcement with respect to unfolding, shielding the enzyme from water molecules by the nearby PEG, and promoting the refolding.[41] It has been shown that PEGylation reduces the water accessible surface area of the protein to protect the intrapeptide hydrogen bonds.[38,39,46] However, the conjugation changes the structure of the resulting biomacromolecule when it is difficult to discriminate the role of the crowding effect.

The PEG stabilizing effect is typically more pronounced for higher PEG concentrations and longer PEG chains if PEG is added to the protein solution.[11,44] The addition of crowders introduces both entropic[47,48] and enthalpic[48,49] contributions affecting the protein stability. Macromolecular crowders, such as PEG, limit the protein's accessible states due to hard-core repulsions since a loss of configurational entropy is typically larger for the protein in the denatured state than that in the folded state. Hence, the hard-core repulsion results in protein stabilization.[49−53] On the other hand, crowders can exhibit either attractive[54] or repulsive soft enthalpic interactions with proteins.[52] Thereby, while entropic contribution typically leads to protein stabilization, an enthalpic contribution can have either stabilizing or destabilizing effect depending on the chemical nature of the crowders and proteins.[52] Overall, either an improvement[50,55,56] or a negative to no effect of crowders on the protein thermal stability[57,58] was observed in experiments depending on the chemical nature of proteins and crowders. For example, the addition of dextran-70 was reported to increase the midpoint temperature of the denaturation curve of LYZ,[59,60] but the presence of PEG[61] and methoxypoly(ethylene glycol)$_{5K}$-*block*-poly(L-aspartic acid sodium salt)$_{10}$[62] resulted in a decrease of the enzyme unfolding temperature. The addition of a block copolymer of PEO and propylene oxide (PPO) resulted in an increase in refolding yield of denatured LYZ. The increased stability in the latter case was explained by hydrophobic interactions between LYZ and PPO blocks, while adding only PEO showed no improvement of thermal stability.[63]

A number of studies of the PEG−LYZ−water phase behavior revealed that the effect of PEG crowders depends on the concentration, molecular mass of PEG, and PEG−LYZ interaction.[64,65] At room temperature, PEG−protein interactions are weak but vary for different proteins. Repulsive protein−protein interactions dominate in dilute aqueous solutions of a low molecular mass PEG. However, the repulsion forces are compensated by the depletion effect with an increase of PEG concentration.[64,65] This PEG concentration effect on protein−protein interactions is inverted at a crowder concentration (C), crossing the transition from dilute to semidilute PEG concentration regime (critical overlap concentration C^*).[58] At $C/C^* > 1$, the protein−protein interactions become more repulsive in the presence of highly entangled PEG coils when the role of the depletion effect decreases.[58] Temperature-dependent PEG−protein soft interactions could prevent the depletion-induced protein aggregation if the depletion forces are compensated by attractive crowder−protein interactions. It was also demonstrated that protein−PEG interactions become more pronounced with increasing the molecular mass of PEG.[66]

In the studies discussed above, LYZ thermal stability in the presence of crowders was limited by monitoring changes in one or other property of the enzyme or phase behavior in

https://doi.org/10.1021/acs.langmuir.1c00872
Langmuir 2021, 37, 8474−8485

solutions. It was rarely combined with monitoring of its catalytic activity. The commonly used characteristic of the thermal stability of proteins is denaturation midpoint temperature (T_m). It is considered that T_m point corresponds to a 50% unfolded state. However, for enzymes, the relationship between thermal stability (T_m) and catalytic activity is nonlinear. Enzymes can lose their catalytic activity even below T_m due to minor conformational changes.[67] It becomes practical to assess enzyme thermal stability via half-life time at a certain temperature.[68]

Herein, a combination of the experimental methods (DLS, SAXS, activity assay analysis, and CD) and MD simulations are utilized to monitor conformational changes of LYZ, PEG, their phase behavior (aggregation) in solutions, and catalytic activity of the enzyme. This combination of methods reveals a dual role of PEG crowders in the improvement of thermal stability of LYZ by (i) delaying of the protein unfolding and (ii) preventing the formation of irreversible LYZ aggregates.

EXPERIMENTAL SECTION

Materials. Lysozyme from chicken egg white (M_w = 14300 g/mol) and polyethylene glycol (M_w = 3350 g/mol (PEG3k) and M_w = 10000 g/mol (PEG10k)) were purchased from Sigma-Aldrich. An EnzChek fluorescence-based lysozyme assay kit (Catalog No. E22013) was purchased from the Thermo Fischer Scientific. *N*-Hydroxysuccinimide-functionalized polyethylene glycol (PEG-NHS) (M_w = 10000 g/mol) was purchased from Nanocs.

Enzyme Solutions. The 0.2 mg/mL LYZ solutions with 0−140 mg/mL PEG3k and 0−60 mg/mL PEG10k were prepared in phosphate-buffered saline (PBS, pH = 7.4). PEG−NHS conjugated LYZ solutions were prepared by mixing 0.2 mg/mL LYZ with 2−50 mg/mL PEG−NHS in PBS. The solutions were incubated overnight at room temperature.

Enzyme Activity, Thermal Stability, and Biocatalytic Kinetics. The enzymatic activity was evaluated after incubation of LYZ in the presence of PEG at the elevated temperature, followed by cooling to room temperature and dilution of the solution to $C/C^* < 1$ for the PEG, since the enzyme activity can be impacted by the concentration regime around of the critical overlap concentration.[69] 60 μL of LYZ and LYZ+PEG solutions were incubated at room temperature or 80 °C for 1 h. The solutions were then diluted 25 times with PBS. Activity and biocatalytic kinetics were measured with EnzCheck lysozyme assay kit in PBS as previously reported.[37]

Circular Dichroism (CD) Spectroscopy. CD studies were performed with a Jasco J-710 spectra polarimeter for LYZ and LYZ +PEG samples by using a quartz cuvette with a path length of 0.1 cm. An enzyme concentration of 15 μM was used for LYZ, LYZ + 60 mg/mL PEG3k, and LYZ + 50 mg/mL PEG10k. The spectra were collected in the far-UV regions from 260 to 190 nm at 1 nm bandwidth. The first spectrum was collected at room temperature; then the sample was heated to 80 °C, and spectra were acquired every 10 min up to 1 h. The sample cell was then cooled to 45 °C, and spectra were acquired every 10 min up to 1 h. Three scans were averaged for each spectrum. The buffer and PEG spectral background were subtracted from the spectra.

Quantification of Lysozyme Aggregation. LYZ and LYZ +PEG solutions were heated at 80 °C for 1 h, followed by filtration with 50 kDa cutoff Amicon ultra-4 centrifugal filters (Millipore UFC805024) after cooling to room temperature. The enzyme concentrations of the filtrates were measured by UV−vis at 280 nm (the extinction coefficient is 38940 cm^{-1} M^{-1}) and compared with original solutions at room temperature. The difference of LYZ concentration prior to heating and after filtration of the aggregate was used to estimate the fraction of aggregated LYZ.

Dynamic Light Scattering of LYZ and PEG Solutions. Dynamic light scattering (DLS) of protein and PEG solutions was analyzed with a Zetasizer Nano-ZS (Malvern Analytical). A 0.2 mg/mL LYZ solution with no PEG, with 60 mg/mL PEG3k, and with 50 mg/mL PEG10k were separately analyzed at 25 and 80 °C (Figure S1).

Molecular Dynamic Simulations. The effect of PEG concentration on the thermal stability of lysozyme was assessed by using atomistic MD simulations at high temperatures. To accelerate the LYZ unfolding, the temperature of 500 K[70−72] was chosen; notably, high-temperature MD simulations are often used to accelerate unfolding.[70,71,73−84] It had been shown that for the two-state proteins the high temperature does not alter the pathway of the unfolding, but only its rate.[76,77] In all simulations at 500 K (NVT ensemble), the density of water was chosen to be equal to that at 300 K.[38,70,72,84] The crystal structure of LYZ was taken from RCSB protein data bank (http://www.rcsb.org, PDB ID 3TXJ). 3TXJ consists of 129 residues; the secondary structure encompasses six α-helices and three stranded antiparallel β-sheets. PEG (degree of polymerization of 21) was constructed and optimized with Gaussian 09 as detailed in our prior studies.[36,85] The CHARMM force fields[86,87] were employed for the protein and PEG.

We fixed the number of PEG chains (237 chains) and varied the number of water molecules (and correspondingly, the size of the simulation box as detailed in the Supporting Information) for different concentrations considered below. The lysozyme and PEG chains were solvated in water (CHARMM TIP3P[88] water model). A NVT ensemble and a V-rescale thermostat were used. All the simulations were performed by using the GROMACS Molecular Dynamics package.[89,90] The LYZ−PEG−water system was first subjected to equilibration and then production runs. Simulation strategies were applied as reported in our previous studies;[36,85] additional details are provided in Supporting Information (Figures S2−S4 and Table S1).

Small-Angle X-ray Scattering (SAXS). SAXS measurements were performed on a custom-built instrument (Saxslab, Amherst, MA) equipped with a copper rotating anode (Bruker AXS) and a 300K Pilatus area detector. We used a 0.6 m nominal sample to detector distance. The actual distance was calibrated with silver behenate. Data reduction was performed with GUISAXS software. Temperature control was performed with an adapted Linkam HFSX350 stage.

Enzyme solutions of 3 mg/mL LYZ and 1.5 mg/mL LYZ with 30 mg/mL PEG3k and 25 mg/mL PEG10k were analyzed with SAXS. The samples were placed in 1 mm diameter capillaries (Charles Supper Company, Natick, MA) and sealed. The exposure time for temperature controlled measurements was kept at 1 h (unless otherwise indicated). We used 0.1°/s for the temperature ramp. The equilibration time at each temperature was set to 2 min. A longer equilibration time was not necessary due to long exposure time. The data fitting was done by using Irena SAXS fitting package[91] (Figures S5 and S6).

RESULTS AND DISCUSSION

Thermal Stability via Catalytic Activity. The effect of PEG on LYZ stability was studied with two PEG crowders, PEG3k (C^* = 122 mg/mL) and PEG10k (C^* = 54.4 mg/mL), at 0−140 and 0−60 mg/mL aqueous solutions, respectively. After incubation at 80 °C for 1 h, native LYZ (control) was denatured with only 15% residual activity. Notably, here and below we refer to native LYZ as LYZ in water only, with no PEG crowders added. The addition of 20 mg/mL of PEG3k resulted in a residual activity of 25%. The thermal stability of LYZ improved with increasing PEG3k concentration by leveling off the PEG concentration effect at 100 mg/mL of PEG3k with about 40% of residual activity (Figure 1a). Adding PEG10k had an even more pronounced stabilizing effect, which was leveled off at 40 mg/mL of PEG with 55% of the residual activity compared to 15% of native LYZ (Figure 1b). The half-life of LYZ in the solutions reveals the thermal stabilization effect of PEG on enzyme catalytic activity. Adding

https://doi.org/10.1021/acs.langmuir.1c00872
Langmuir 2021, 37, 8474−8485

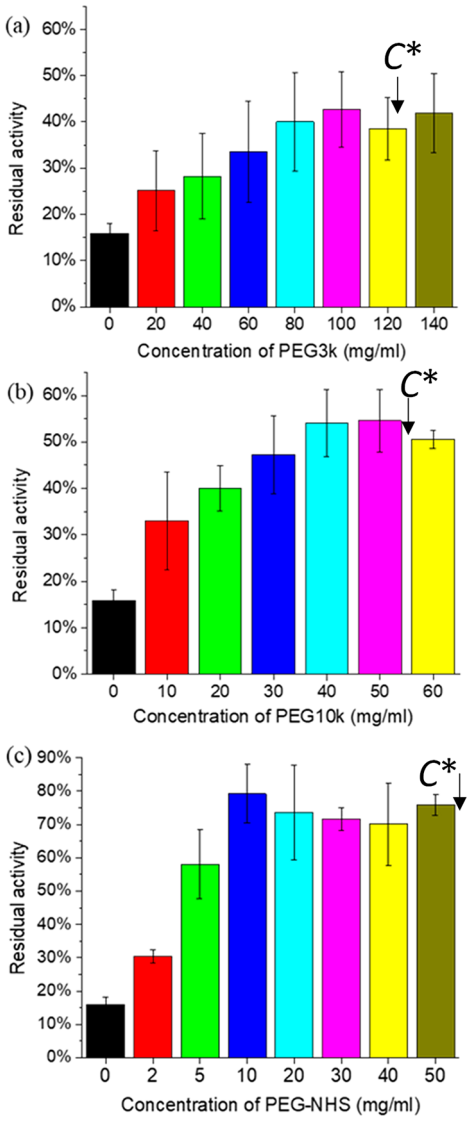

Figure 1. Residual activity of LYZ and LYZ with different concentrations of (a) PEG3k, (b) PEG10k, and (c) PEG−NHS after 1 h incubation at 80 °C.

PEG extends the half-life of LYZ at 80 °C from 20.5 min to 28.6 min and 48.2 min for PEG3k and PEG10k solutions, respectively (Table 1 and Figure S7).

For reference, we analyzed the thermal stability of LYZ covalently conjugated to PEG−NHS ester (M_w = 10000 g/mol). The thermal stability of LYZ was improved up to 80% of the residual activity with only 10 mg/mL of PEG in solution (Figure 1c). This result evidently demonstrated the critical role of PEG−protein interactions for the thermal stabilization of the protein when the depletion effect is overcome by the covalent conjugation. In the latter case, the stabilization was approached at a PEG concentration significantly below the critical overlap concentration C^*, while a similar stabilizing effect for noncovalently conjugated PEG is approached at ratios C/C^* close to 1.

The Michaelis−Menten kinetic model was used to analyze biocatalytic kinetics for the native LYZ and LYZ+PEG mixtures (Table 1). The LYZ+PEG solutions were prepared at PEG concentrations C close to C^*. After 1 h incubation at 80 °C, the samples were cooled to room temperature and 25-fold diluted to C significantly below C^*. In the reference experiment, the same sequence of steps was performed with no heating and incubation at 80 °C. At room temperature, both PEG3k and PEG10k solutions showed higher K_M (lower affinity) compared to the native LYZ. This indicated a steric hindrance of the LYZ reactive sites by PEG. The lower affinity was compensated by greater turnover numbers (k_{cat}) for LYZ +PEG due to the increased biocatalytic activity of the active sites of the enzyme. The boost of catalytic activity was stronger for PEG10k. The steric hindrance and increased activity of catalytic sites compensated each other so that k_{cat}/K_M remained unchanged for all samples. However, the steric hindrance and increased catalytic activity both demonstrate soft PEG−LYZ interactions even in dilute solutions, when PEG10k interacts with LYZ stronger than PEG3k, which is in good agreement with the results published elsewhere.[69]

The kinetic characteristics evaluated after 1 h incubation at 80 °C revealed that the PEG−LYZ interaction provided thermal stabilization of the protein with the same tendency but a stronger effect of PEG10k than PEG3k. The enzyme catalytic activity dropped after the heating because of denaturing. However, the loss of activity was substantially lower in the presence of PEG as can be concluded by comparing k_{cat} and k_{cat}/K_M for the samples (Table 1).

Thermal Stability via LYZ Conformational Changes. The information about the conformational states of LYZ and LYZ+PEG was collected by using CD spectra. CD spectra were first acquired at 25 °C. Then the samples were heated to 80 °C, and CD spectra were acquired every 10 min of the 1 h heating time. The sample was then cooled to 45 °C, and the data were acquired every 10 min of the 1 h cooling step. CD spectra showed unfolding of the enzyme during heating to 80 °C, and a fractional recovering of the conformation after cooling down, indicating refolding of LYZ at lower temperatures (Figure 2). The secondary structures of LYZ in these samples were analyzed by using the BeStSel online computer program[92,93] (Figure 3). Native LYZ showed a decrease in both helix 1 and 2 structures at elevated temperatures as the result of LYZ unfolding. The helix 2 structure was partially recovered after cooling, but the helix 1 retained in the unfolded

Table 1. Kinetic Constants and Half-Life of LYZ and LYZ+PEG Solutions

	room temperature				80 °C, 1 h				
sample	V_{max} (nM/min)	K_M (nM)	k_{cat} ($\times 10^{-4}$ s^{-1})	k_{cat}/K_M ($\times 10^4$ M^{-1} s^{-1})	V_{max} (nM/min)	K_M (nM)	k_{cat} ($\times 10^{-4}$ s^{-1})	k_{cat}/K_M ($\times 10^4$ M^{-1} s^{-1})	half-life at 80 °C (±1 min)
LYZ	11.65 ± 0.38	28.40 ± 0.28	3.50	1.23	0.64 ± 0.15	33.75 ± 0.13	0.19	0.06	20.5
LYZ +PEG3k	14.01 ± 0.65	31.44 ± 0.52	4.20	1.34	1.97 ± 0.23	34.32 ± 0.20	0.59	0.17	28.6
LYZ +PEG10k	18.99 ± 0.55	44.68 ± 0.46	5.70	1.28	3.93 ± 0.38	21.11 ± 0.29	1.18	0.56	48.2

https://doi.org/10.1021/acs.langmuir.1c00872
Langmuir 2021, 37, 8474−8485

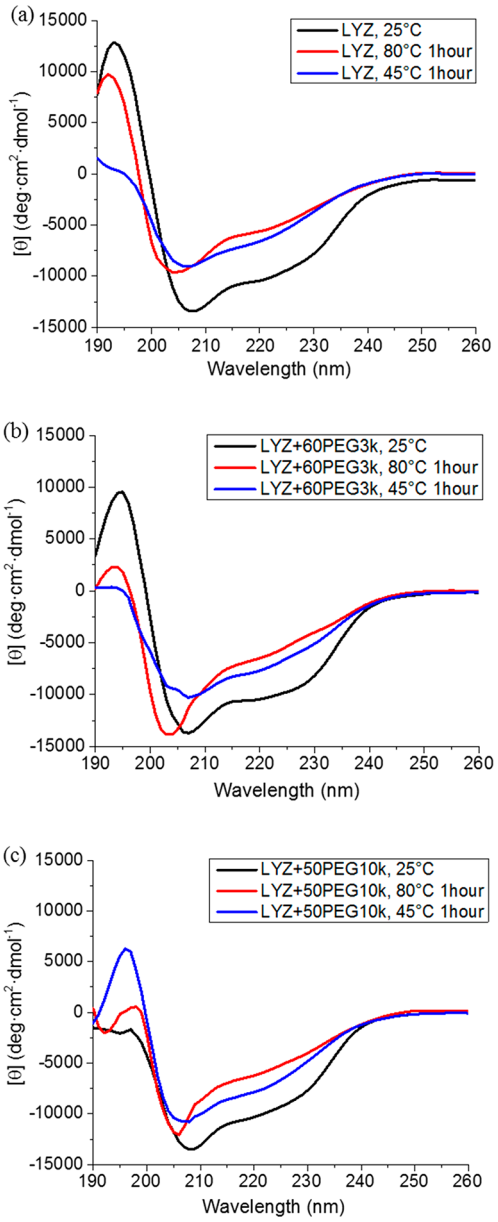

Figure 2. CD spectra of (a) LYZ, (b) LYZ+PEG3k (60 mg/mL), and (c) LYZ+PEG10k (50 mg/mL) at various temperatures.

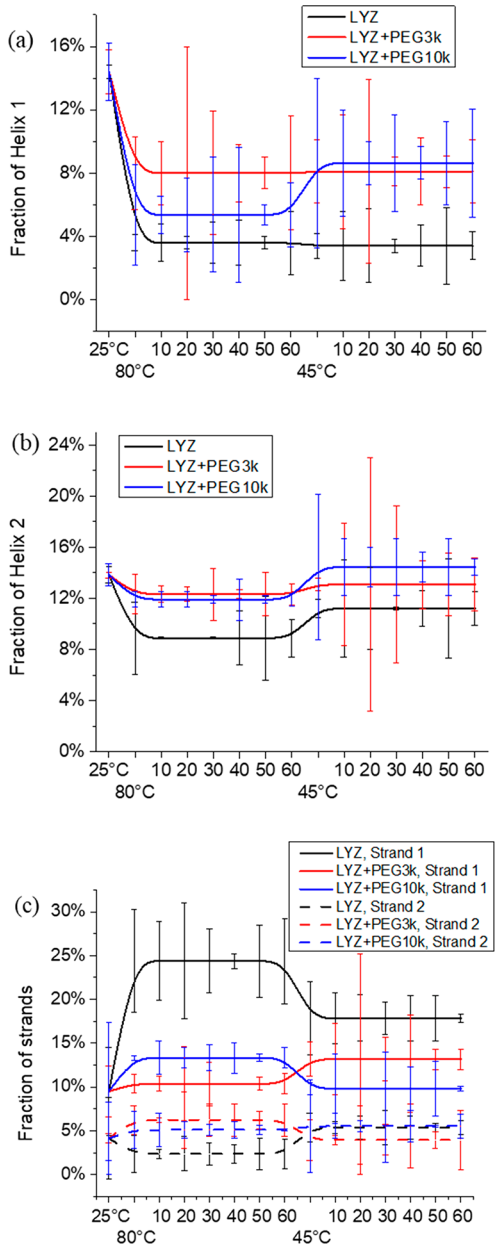

Figure 3. Fraction of secondary structure (a) helix 1, (b) helix 2, and (c) strands for LYZ vs LYZ+PEG.

conformation, which implied that the secondary structure was not fully recovered to the original state (Figure 3a,b). This change explains the observed loss of enzyme activity (Figure 1 and Table 1).

With the addition of both PEG3k and PEG10k, the helix structures were also partially denatured at 80 °C, but with much lower margins compared to the LYZ only. After cooling to 45 °C, the helix portion recovered to much higher fraction than that for LYZ (Figure 3a,b), which was consistent with the LYZ catalytic activity tests results, where the introduction of PEG could stabilize LYZ at the elevated temperature (Figure 1 and Table 1). A lower fraction of thermally generated strands for LYZ+PEG compared to LYZ (Figure 3c) explains that the presence of PEG could reduce LYZ aggregation due to blocking the conformational changes that lead to the formation of β-sheets. The formation of β-sheets is known to favor a possible aggregation[63,94] and as an indication of enzyme denaturation.[95]

Thermal Stability via LYZ Aggregation Characterization. Thermal denaturing of LYZ develops by unfolding and aggregation stages. We estimated the hydrodynamic diameter (D_H) of LYZ, LYZ aggregates, and LYZ+PEG associates at 25 and 80 °C using DLS. For LYZ, D_H = 3.1 nm as estimated with DLS at room temperature. A rapid aggregation of LYZ was observed at 80 °C, where the D_H was increased to about 212 nm (Table 2). For PEG, the DLS estimated D_H was close to that of LYZ. Practically, these two molecules could not be discriminated by using DLS in solutions containing LYZ+PEG (Figure S1). However, after incubation of LYZ+PEG solutions at 80 °C, DLS revealed two different sizes of the scattering particles with D_H = 3.2 nm and about 164 nm in the presence of PEG3k and 4.1 nm and about 208 nm in the presence of PEG10k (Table 2).

LYZ and LYZ+PEG solutions incubated at 80 °C were filtered by using 50 kDa cutoff filters once cooled to room

https://doi.org/10.1021/acs.langmuir.1c00872
Langmuir 2021, 37, 8474−8485

Table 2. LYZ Dimensions at 25 and 80 °C and Fraction of Irreversible Aggregates of LYZ vs LYZ+PEG after 1 h Incubation at 80 °C

	D_H (nm)		
sample	25 °C	80 °C	irreversible aggregation of LYZ (%)
LYZ	3.1 ± 0.8	211.8 ± 33.0	84 ± 6
LYZ +PEG3k	3.4 ± 0.7	3.2 ± 0.4; 163.8 ± 15.3	58 ± 9
LYZ +PEG10k	3.9 ± 0.7	4.1 ± 0.4; 208.4 ± 53.8	42 ± 11
PEG3k	2.5 ± 0.6	3.3 ± 0.7	NA
PEG10k	3.8 ± 0.5	5.2 ± 0.3	NA

temperature. The filtrate contained nonaggregated LYZ. Its concentration was estimated with UV−vis spectra to calculate fractions of aggregated LYZ during the high-temperature incubation. The results revealed that 84% of native LYZ, 58% LYZ in the presence of PEG3k, and 42% LYZ in the presence of PEG10k formed irreversible aggregates (Table 2).

LYZ and LYZ+PEG solutions were probed with SAXS. All experiments were conducted at PEG concentrations below the critical overlap concentration to minimize the impact of scattering from PEG. X-ray scattering for LYZ was satisfactorily fitted with a spherical particle model, $2R_g$ = 3.6 nm, with a narrow size distribution approaching zero (Table 3). Upon

Table 3. SAXS Fitted Results for LYZ and LYZ+PEG Aqueous Solution

			aggregation of LYZ (±5%)	
sample	temp (°C)	$2R_g$ (±0.1 nm)	SAXS	filtration experiment
LYZ	25	3.6	0	0
	80	4.2	65	NA
	cooling to 25 °C after heating	4.2	78	84
LYZ +PEG3k	25	3.5	0	0
	80	4.8	NA	NA
	cooling to 25 °C after heating	4.2	74	79
LYZ +PEG10k	25	3.5	0	0
	80	3.6; 7.6	NA	NA
	cooling to 25 °C after heating	3.2; 6	59	71

heating to 80 °C, the scattering showed both an increase in the particle size, which could be attributed to a partial unfolding, and an increase in the particle polydispersity to about 27% (Gaussian distribution), which decreased to 12% when the sample was brought back to room temperature. The upturn in the scattering intensity at scattering vectors below 0.03 A^{-1} was indicative of aggregation (Figure 4a); however, at the measured scattering vector range, we could not obtain the quantitative measurement of aggregate sizes or structure. On the basis of the scattering intensity change with the temperature at low Q, at the plateau region, and assuming a constant scattering contrast of lysozyme, we estimated that only ∼22% of the enzyme remained in the solution in the nonaggregated form upon cooling to 25 °C after heating.

A solution of 25 mg/mL PEG10k stabilized LYZ even after 3 h of incubation time at 80 °C. After cooling from 80 to 25 °C, the scattering profile showed only small changes compared to the native LYZ at room temperature (Figure 4c). However, change in morphology was more pronounced at 80 °C, likely due to partial unfolding. Unlike scattering profiles in Figures 4a, when the scattering signal was exclusively originating from LYZ, the scattering data in Figure 4b,c represented contributions from both LYZ and PEG, with PEG contributing about 30% to the total signal. Interestingly, at room temperature, the mathematical sum of the scattering from separate LYZ and PEG solutions and the scattering from the LYZ and PEG mixture, while very similar, showed subtle deviations that may indicate either small conformational changes of LYZ in PEG solutions or interactions of PEG with LYZ surface. To delineate these two effects, additional studies using neutron scattering may be required.

PEG3k at 30 mg/mL also provided some improvement to LYZ thermal stability (Figure 4b), albeit to a much smaller degree than PEG10k. After the heating and cooling cycle, only about 26% of free enzyme remained (estimated from the relative intensity at low Q and corrected for PEG3k contribution to scattering), in contrast to 22% of LYZ and 41% of LYZ+PEG10k in PBS solution (Table 3).

Similar to the model for LYZ in PBS solution, the SAXS data for LYZ in the presence of PEG can be fitted by using the model of spheroidal particles with Gaussian size distribution. The PEG contribution to the scattering was taken into account for the fitting (Figure S5). However, unlike LYZ in PBS, LYZ in PEG produced significantly better fit results when LYZ was modeled with elongated spheroidal particles instead of spherical particles (Figure S6). In addition, for LYZ in PEG10k, it was necessary to use two populations of particles to model the scattering data upon heating.

With SAXS, we probed changes of the PEG conformation with temperature (Figure 4d). At 80 °C, the scattering intensity increased at small scattering vectors, indicating the presence of larger particles in the solution, which indicated a slight association between PEG molecules (Table 4). This association was fully reversible with the temperature (not shown).

SAXS experiments with PEG solutions demonstrated the tendency for PEG aggregation with temperature (Figure 4d and Table 4), indicating that water becomes a progressively poorer solvent. The sizes of the PEG molecules aggregates are small. We did not observe macroscopic phase separation or precipitation of larger aggregates because the experiment was conducted at the temperature well below the PEG lower critical solution temperature (LCST is around 150 °C for PEG3k and 110 °C for PEG10k).[96] This tendency was better pronounced for PEG10k than for PEG3k, which is in good agreement with DLS, CD spectra, and activity assay tests. We observed a strong irreversible aggregation of LYZ at the elevated temperature, while the aggregation was partially reversible for LYZ+PEG3k and LYZ+PEG10k solutions, where the stabilizing effect of PEG10k was much stronger than that of PEG3k.

MD Simulations of LYZ−PEG−H_2O: Effect of PEG Concentration in the Vicinity of LYZ. MD simulations were performed to probe the effect of PEG concentration on the thermal stability of LYZ. We only focused on the dynamics in the close vicinity of a single LYZ. PEG chains in simulations were significantly shorter than those used in the experiments. It had been previously shown that the long PEG chains exhibit partially amphiphilic (instead of hydrophilic) character at

https://doi.org/10.1021/acs.langmuir.1c00872
Langmuir 2021, 37, 8474−8485

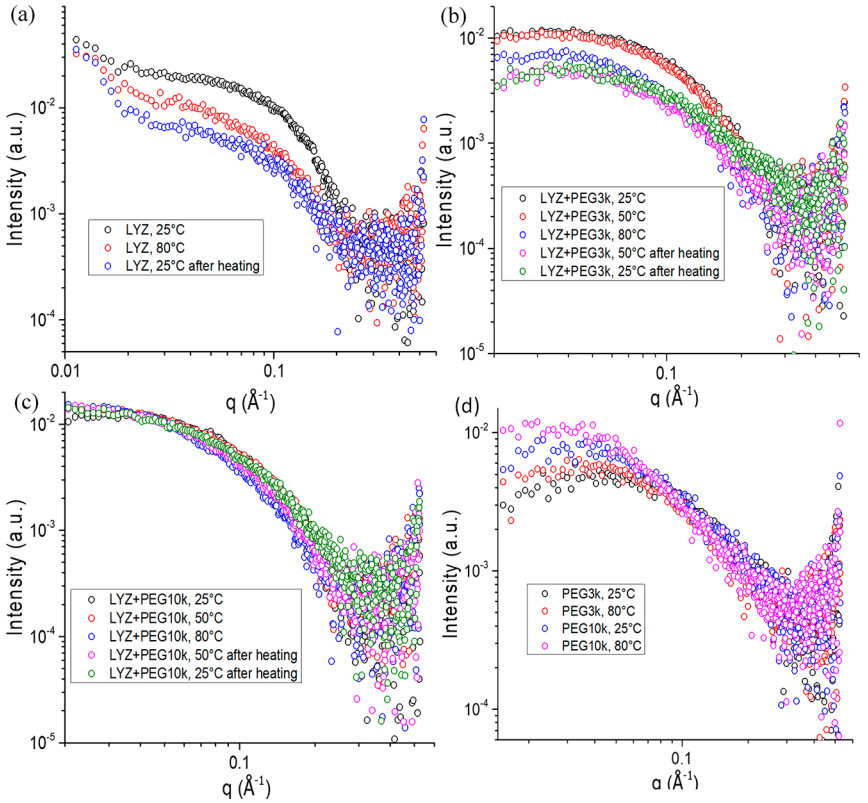

Figure 4. SAXS data for LYZ, LYZ+PEG, and PEG solutions at different temperatures. (a) 3 mg/mL LYZ at 25 and 80 °C; 1.5 mg/mL LYZ with (b) 30 mg/mL PEG3k, and (c) 25 mg/mL PEG10k at 25, 50, and 80 °C. Samples were kept for 1 h at each temperature point for (a) and 3 h for (b) and (c). (d) SAXS data of 60 mg/mL PEG3k and 50 mg/mL PEG10k at 25 and 80 °C.

Table 4. PEG $2R_g$ Extracted from Guinier−Porod Fits

sample	$2R_g$ (±0.1 nm)
PEG3k, 25 °C	2.4
PEG3k, 80 °C	3.0
PEG10k, 25 °C	3.4
PEG10k, 80 °C	4.6

ambient temperatures and thereby interact with proteins.[66,97] To mimic the effect of the longer PEG chains used in experiments and their interactions with proteins,[66,97] a range of relatively high concentrations of PEG was chosen in our simulation studies. Specifically, we chose the systems with three concentrations of PEG in water (90%, 80%, and 50% w/w of PEG) at high temperature (500 K). In each independent simulation run, we calculated the time evolution of a root-mean-square deviation (RMSD) of LYZ with respect to its initial state and the number of intraprotein hydrogen bonds (H-bonds). The RMSD at each moment of time is defined as $\mathrm{RMSD}(t) = \left[\frac{1}{N}\sum_{i=1}^{N}(\mathbf{r}_i(t) - \mathbf{r}_i(0))^2\right]^{1/2}$, where $\mathbf{r}_i(t)$ and $\mathbf{r}_i(0)$ are the coordinates of the backbone C_α atom i at a time t and at initial time, respectively, and N is the total number of C_α atoms in the backbone. While calculating RMSD, we performed the rotational and translational superposition of the center of mass of the LYZ with respect to its initial structure. RMSD quantifies the deviation of LYZ conformation from its initial conformation; an increase in RMSD indicates unfolding of the protein globule. Notably, in nonequilibrium simulations, the stability of the enzyme can be related to the response time after the external perturbing stimulus, such as high temperature, is applied: the slower the enzyme reacts to the perturbing forces, the more stable it is.[101]

For native LYZ at high temperature, a sharp increase in RMSD (Figure 5a, black curve) and a corresponding decrease in the number of intraprotein H-bonds (Figure 5b) indicated a strong structural deviation from its initial structure due to the unfolding. Notably, in LYZ−PEG systems at T = 300 K, the LYZ crystal structure remained stable, similar to that of pure LYZ at room temperature (Figure S2). With the addition of 90% w/w of PEG chains (the highest concentration considered), both RMSD and the number of H-bonds showed that LYZ retained its secondary structures at high temperatures (Figures 5a,b, red curves). The DSSP (Dictionary of Secondary Structure in Proteins) analysis (Figure 5c) and a simulation snapshot (Figure 5e) confirmed that the secondary structures remained mainly intact in the simulation runs with the highest concentration of PEG (90% w/w). Specifically, the α-helices (blue horizontal stripes) and β-sheets (red horizontal stripes) remained largely intact during the entire simulation run (Figure 5c) with relatively small deviations from that for native LYZ at room temperature (Figure S2). For the remaining cases, with the decrease in the concentration of PEG chains, the deviations of the secondary structures were clearly observed via the increase of RMSD (Figure 5a) and the decrease of the number of intraprotein H-bonds (Figure 5b). The DSSP analysis (Figure 5d) and a simulation snapshot (Figure 5f) confirmed that LYZ secondary structures were strongly disrupted at early times and completely lost at 150 ns with 50% of PEG as evident from the disappearance of the α-helices (blue horizontal stripes) and β-sheets (red horizontal stripes) by this time instant in DSSP plots in Figure 5d. In all

https://doi.org/10.1021/acs.langmuir.1c00872
Langmuir 2021, 37, 8474−8485

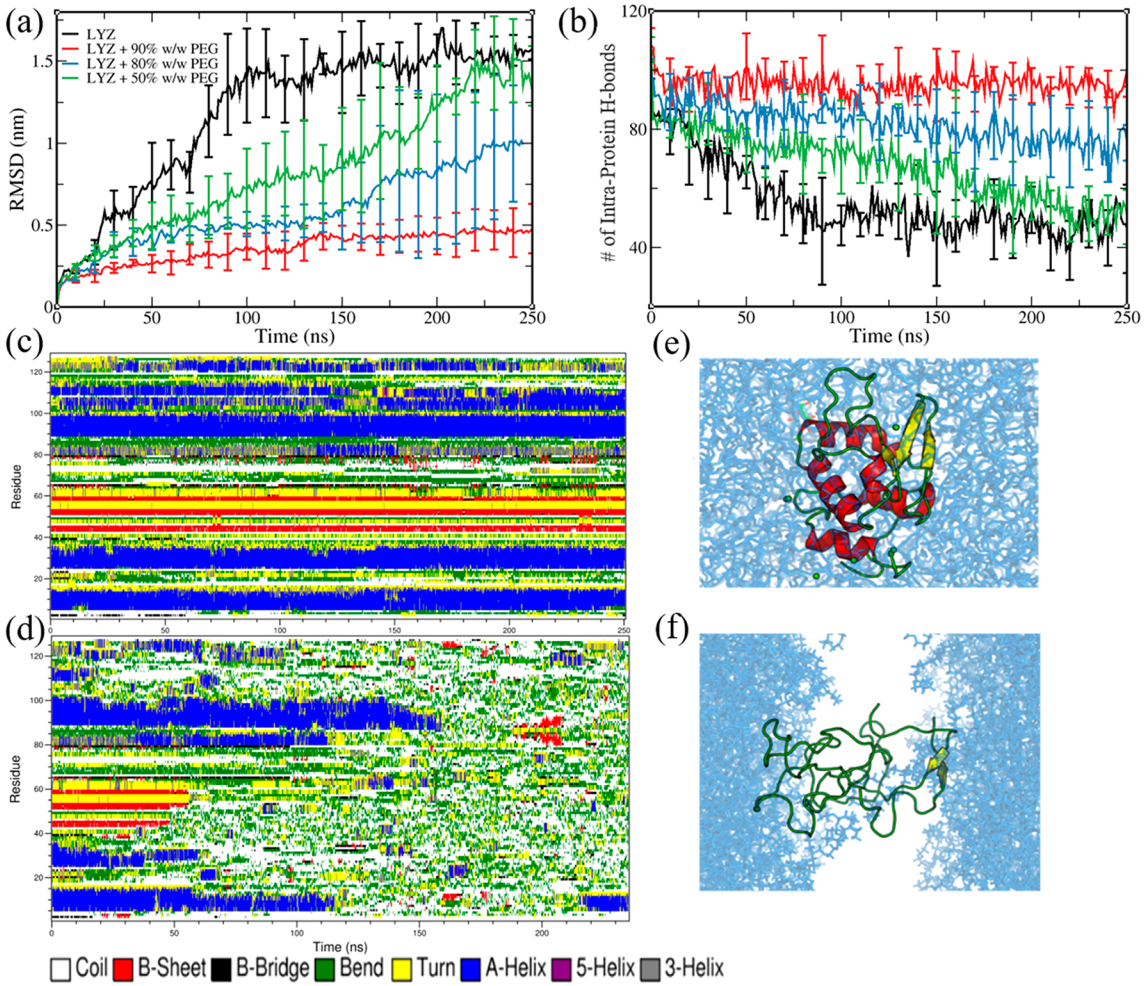

Figure 5. MD simulations. Time evolution of (a) RMSD and (b) number of intraprotein H-bonds at T = 500 K for the native LYZ (black line) and LYZ with different concentrations of PEG chains as given in the legend (red/blue/green for 90%/ 80%/ 50% of PEG). The data are averaged over four independent simulation runs. DSSP plots for lysozyme with 90% w/w of PEG in (c) and 50% w/w of PEG in (d). Snapshots in the vicinity of lysozyme with 90% w/w of PEG in (e) and 50% w/w PEG in (f) at late times (250 ns). Only a portion of the simulation box is shown for clarity in (e) and (f); PEG chains are shown in blue, and water molecules are hidden. Entire simulation boxes are depicted in the Supporting Information.

cases in PEG-LYZ simulations, the unfolding time significantly exceeded that of pure LYZ (black curves in Figures 5a,b), indicating that the addition of PEG resulted in stabilizing the secondary structures of the enzyme for a limited time, with the more pronounced effect at higher PEG concentrations.

Notably, the error bars for RMSD and for the number of intraprotein H-bonds (Figure 5a,b) are relatively small for 90% of PEG, indicating similar dynamics in all independent simulation runs. On the contrary, the error bars are large for the remaining concentrations, indicating that unfolding occurred at distinctly different time instants. Representative examples of time evolution in independent simulation runs are shown in Figure S3. The simulation results in Figure 5 show that the addition of PEG could preserve the secondary structure of the enzyme to some degree for a limited time. This effect increases with an increase in PEG concentration, while only at the highest concentration in the close vicinity of the lysozyme (red curves in Figure 5a,b) is the stabilization of the secondary structures of LYZ at elevated temperatures observed.

The reason for thermal stabilization of a single lysozyme at a high concentration of PEG can be understood by comparing the simulations snapshots for the highest (Figure 5e) and lowest (Figure 5f) concentrations of PEG considered in simulations. At late times a single pure water domain containing LYZ (Figure 5f) and another domain that mainly containing PEG were formed. An onset of unfolding corresponded to LYZ located within the water domain (Figure S4). At the high temperatures chosen herein to model unfolding, we observed the phase separation between PEG and water for a range of concentrations of PEG (80% and 50% w/w). The hydrophobic character of PEG in our simulations was consistent with prior studies that showed that at sufficiently high temperatures PEG became immiscible with water.[96,98−100] Specifically, it had been shown that there is an enhancement of hydrophobicity for shorter PEG chains at elevated temperatures;[97] similar dehydration behavior had been reported for long PEG chains.[96,98−100] For the highest concentration of PEG (90% w/w), we no longer observed phase separation, and the LYZ was buried within PEG (Figure 5e). Hence, our results showed that lysozyme's thermal denaturation is prevented, and the secondary structures remain largely intact due to the reduced water access for the sufficiently high concentration of PEG in the vicinity of the enzyme. These results are consistent with prior studies that showed that reducing the accessibility of water to

https://doi.org/10.1021/acs.langmuir.1c00872
Langmuir 2021, 37, 8474−8485

proteins[41,46,85,102] or using organic solvents instead of water[103] results in significant improvement of their stability at high temperatures.

CONCLUSIONS

We utilized a combination of the experimental methods and MD simulations to characterize conformational changes of LYZ and their aggregation in PEG solutions. The activity assay proves that native LYZ denatures at 80 °C, pH 7.4, with only 15% of residual activity after 1 h incubation (Figure 1 and Table 1). CD spectra showed that in the latter case LYZ irreversibly lost an essential fraction of the secondary structure elements forming a larger fraction of strands favoring protein aggregation due to the hydrophobic effect (Figures 2 and 3). DLS and SAXS confirmed the irreversible formation of large aggregates that consumed about 80% of LYZ (Figure 4, Tables 2 and 3).

PEG was used as a crowder additive. PEG aqueous solutions are characterized by LCST typically exceeding 100 °C.[96] While no macroscopic phase separation was observed in our experiments, water becomes progressively poor solvent with temperature increase from room temperature to the temperature of the experiments, 80 °C. This change in solvent quality resulted in more compact PEG coils and the formation of their small aggregates due to the hydrophobic effect. The aggregation effect was more pronounced with an increase of the molecular mass of PEG. This was supported by SAXS experiments (Figure 4d and Table 4).

The analysis of the biocatalytic reaction kinetics at room temperature showed some decrease of LYZ−substrate affinity but an increase of the reaction turnover at the same time (Table 1). These changes can be explained by PEG−LYZ soft interactions. The formation of LYZ−PEG associates was detected with DLS and SAXS experiments via increase in particle size (Tables 2 and 3).

The temperature-driven formation of LYZ aggregates in PEG solutions was observed with both DLS and SAXS at 80 °C (Tables 2 and 3, Figure 4). The analysis based on filtration of the aggregates showed that about 50% of LYZ was irreversibly aggregated with the addition of PEG (compare with 80% for native LYZ). In SAXS experiments, we detected by size the presence of three different particle populations: about 3.5 nm, 6 nm, and large aggregates. We associate these particles with LYZ, PEG−LYZ reversible aggregates, and LYZ−LYZ irreversible aggregates. The amount of LYZ consumed by the irreversible aggregates was about 59% as estimated by SAXS for 25 mg/mL PEG10k compared to 71% of the filtration experiment. This difference may be attributed to the fact that estimates of aggregation using SAXS are based on the assumption that after cooling the scattering originates only from nonaggregated LYZ with no changes in its conformation. Thus, the extent of aggregation may be underestimated if there is an unquantified contribution of larger aggregates to the total scattering.

CD spectra confirmed changes in the secondary structures of LYZ in the presence of PEG, but these changes were less expressed as compared to the control and some of the conformational changes recovered after cooling the samples (Figures 2 and 3). Such partial and reversible unfolding was also observed in SAXS measurements at 80 °C (Figure 4 and Table 3). The results were in good agreement with the residual catalytic activity of LYZ in the presence of PEG (Figure 1 and Table 1).

MD simulations also demonstrated much smaller changes of LYZ secondary structures at high temperatures in the presence of PEG. Specifically, simulations showed that a more hydrophobic PEG shell in the close vicinity of the LYZ reduces water molecule access to the LYZ globule. The simulation results indicated that the addition of PEG could preserve the secondary structure of the enzyme to some degree for a limited time; the effect was more pronounced with an increase in PEG concentration (Figure 5). Notably, only at the highest concentration in the close vicinity of the enzyme the secondary structures of LYZ were stabilized to a high degree at elevated temperatures. The PEG concentrations considered in simulations were chosen to be significantly higher than those in experiments since much shorter polymer chains were considered in the close vicinity of the single enzyme. Hence, simulations confirm that the addition of PEG chains contributes to the stabilization of the secondary structures; the effect is more pronounced with the increase in PEG concentration.

The biocatalytic activity experiments provided evidence for a strong effect of PEG concentration. Residual activity after heating increased with PEG concentration and then leveled off at the critical overlap concentration. The effect of PEG molecular mass was monitored by using different methods. The residual catalytic activity (Figure 1 and Table 1) and PEG aggregation (Table 4) after heating were greater, while LYZ conformational changes (Figures 2 and 3) and LYZ aggregation (Tables 2 and 3) were less pronounced with an increase of PEG molecular mass. The possible interpretation of this result is that with increasing molecular mass PEG becomes more hydrophobic and interacts more strongly with LYZ.

Covalent conjugation of LYZ with PEG−NHS demonstrated high efficiency of the conjugates in terms of thermal stabilization and residual activity (Figure 1c). This reference experiment underlines the importance of LYZ−PEG interactions for preventing LYZ denaturing and aggregation. The stabilizing effect of PEG is approached at much lower PEG concentrations in the case of covalent PEGylation.

On the basis of the analysis of the obtained results, we may draw general conclusions about the crowding effect in protein−PEG−water solutions on protein thermal stability. With an increase in temperature, PEG becomes more hydrophobic; this tendency is stronger for a higher molecular mass of PEG and concentration. The PEG−protein association has a dual effect on thermal stabilization. First, the PEG−protein interaction reduces the depletion attraction between protein globules and minimizes irreversible protein aggregation. Our results show that the stabilizing effect of PEG saturates at the critical overlap concentration. Second, the formation of a PEG shell due to the PEG−protein hydrophobic interactions results in preventing the access of water molecules to the protein globule at elevated temperature, hence delaying protein denaturing.

ASSOCIATED CONTENT

Supporting Information

The Supporting Information is available free of charge at https://pubs.acs.org/doi/10.1021/acs.langmuir.1c00872.

A dynamic light scattering figure of enzyme solutions, additional details about molecular dynamics simulations, and small-angle X-ray scattering data fitting (PDF)

https://doi.org/10.1021/acs.langmuir.1c00872
Langmuir 2021, 37, 8474−8485

AUTHOR INFORMATION

Corresponding Author

Sergiy Minko − *Nanostructured Materials Lab, University of Georgia, Athens, Georgia 30602, United States;* orcid.org/0000-0002-7747-9668; Email: sminko@uga.edu

Authors

Xue Wang − *Nanostructured Materials Lab, University of Georgia, Athens, Georgia 30602, United States*

Jeremy Bowman − *Nanostructured Materials Lab, University of Georgia, Athens, Georgia 30602, United States*

Sidong Tu − *Department of Materials Science and Engineering, Clemson University, Clemson, South Carolina 29634, United States*

Dmytro Nykypanchuk − *Center for Functional Nanomaterials, Brookhaven National Laboratory, Upton, New York 11973, United States*

Olga Kuksenok − *Department of Materials Science and Engineering, Clemson University, Clemson, South Carolina 29634, United States;* orcid.org/0000-0002-1895-5206

Complete contact information is available at: https://pubs.acs.org/10.1021/acs.langmuir.1c00872

Notes

The authors declare no competing financial interest.

ACKNOWLEDGMENTS

The authors acknowledge the support of the National Science Foundation USA Award 1604526 and the National Science Foundation EPSCoR Program Award OIA-1655740. O.K. and S.T. thank Chandan K. Choudhury for valuable discussions. Clemson University is acknowledged for compute time on Palmetto cluster. This research, in part, used resources of the Center for Functional Nanomaterials, which is a U.S. DOE Office of Science Facility, at Brookhaven National Laboratory under Contract DE-SC0012704.

REFERENCES

(1) Ansari, S. A.; Husain, Q. Potential applications of enzymes immobilized on/in nano materials: A review. *Biotechnol. Adv.* **2012**, *30* (3), 512−23.

(2) Ariga, K.; Ji, Q.; Mori, T.; Naito, M.; Yamauchi, Y.; Abe, H.; Hill, J. P. Enzyme nanoarchitectonics: organization and device application. *Chem. Soc. Rev.* **2013**, *42* (15), 6322−45.

(3) Es, I.; Vieira, J. D.; Amaral, A. C. Principles, techniques, and applications of biocatalyst immobilization for industrial application. *Appl. Microbiol. Biotechnol.* **2015**, *99* (5), 2065−82.

(4) Kirk, O.; Borchert, T. V.; Fuglsang, C. C. Industrial enzyme applications. *Curr. Opin. Biotechnol.* **2002**, *13* (4), 345−351.

(5) Min, K.; Yoo, Y. J. Recent progress in nanobiocatalysis for enzyme immobilization and its application. *Biotechnol. Bioprocess Eng.* **2014**, *19* (4), 553−567.

(6) Misson, M.; Zhang, H.; Jin, B. Nanobiocatalyst advancements and bioprocessing applications. *J. R. Soc., Interface* **2015**, *12* (102), 20140891.

(7) Khamari, L.; Pramanik, U.; Shekhar, S.; Mohanakumar, S.; Mukherjee, S. Thermal Reversibility and Structural Stability in Lysozyme Induced by Epirubicin Hydrochloride. *Langmuir* **2021**, *37* (11), 3456−3466.

(8) Arakawa, T.; Prestrelski, S. J.; Kenney, W. C.; Carpenter, J. F. Factors affecting short-term and long-term stabilities of proteins. *Adv. Drug Delivery Rev.* **1993**, *10* (1), 1−28.

(9) Bischof, J. C.; He, X. Thermal stability of proteins. *Ann. N. Y. Acad. Sci.* **2005**, *1066* (1), 12−33.

(10) Daniel, R. M. The upper limits of enzyme thermal stability. *Enzyme Microb. Technol.* **1996**, *19* (1), 74−79.

(11) Iyer, P. V.; Ananthanarayan, L. Enzyme stability and stabilization—Aqueous and non-aqueous environment. *Process Biochem.* **2008**, *43* (10), 1019−1032.

(12) Schulz, G. E.; Schirmer, R. H. *Principles of Protein Structure*; Springer Science & Business Media: New York, 2013; p 320.

(13) Hummer, G.; Garde, S.; García, A. E.; Pratt, L. R. New perspectives on hydrophobic effects. *Chem. Phys.* **2000**, *258* (2), 349−370.

(14) Kazlauskas, R. Engineering more stable proteins. *Chem. Soc. Rev.* **2018**, *47* (24), 9026−9045.

(15) Arnold, F. H. Directed Evolution: Bringing New Chemistry to Life. *Angew. Chem., Int. Ed.* **2018**, *57* (16), 4143−4148.

(16) Badenhorst, C. P. S.; Bornscheuer, U. T. Getting Momentum: From Biocatalysis to Advanced Synthetic Biology. *Trends Biochem. Sci.* **2018**, *43* (3), 180−198.

(17) Rothlisberger, D.; Khersonsky, O.; Wollacott, A. M.; Jiang, L.; DeChancie, J.; Betker, J.; Gallaher, J. L.; Althoff, E. A.; Zanghellini, A.; Dym, O.; Albeck, S.; Houk, K. N.; Tawfik, D. S.; Baker, D. Kemp elimination catalysts by computational enzyme design. *Nature* **2008**, *453* (7192), 190−5.

(18) Gauthier, M. A.; Klok, H.-A. Polymer−protein conjugates: an enzymatic activity perspective. *Polym. Chem.* **2010**, *1* (9), 1352−1373.

(19) Hwang, E. T.; Gu, M. B. Enzyme stabilization by nano/microsized hybrid materials. *Eng. Life Sci.* **2013**, *13* (1), 49−61.

(20) Zheng, G.; Liu, S.; Zha, J.; Zhang, P.; Xu, X.; Chen, Y.; Jiang, S. Protecting enzymatic activity via zwitterionic nanocapsulation for the removal of phenol compound from wastewater. *Langmuir* **2019**, *35* (5), 1858−1863.

(21) Ma, X.; Sui, H.; Yu, Q.; Cui, J.; Hao, J. Silica Capsules Templated from Metal−Organic Frameworks for Enzyme Immobilization and Catalysis. *Langmuir* **2021**, *37* (10), 3166−3172.

(22) Pelegri-O'Day, E. M.; Lin, E.-W.; Maynard, H. D. Therapeutic protein−polymer conjugates: advancing beyond PEGylation. *J. Am. Chem. Soc.* **2014**, *136* (41), 14323−14332.

(23) Gonen-Wadmany, M.; Oss-Ronen, L.; Seliktar, D. Protein−polymer conjugates for forming photopolymerizable biomimetic hydrogels for tissue engineering. *Biomaterials* **2007**, *28* (26), 3876−3886.

(24) Masschalck, B.; Michiels, C. W. Antimicrobial properties of lysozyme in relation to foodborne vegetative bacteria. *Crit. Rev. Microbiol.* **2003**, *29* (3), 191−214.

(25) Guez, V.; Roux, P.; Navon, A.; Goldberg, M. E. Role of individual disulfide bonds in hen lysozyme early folding steps. *Protein Sci.* **2002**, *11* (5), 1136−1151.

(26) Lumry, R.; Eyring, H. Conformation changes of proteins. *J. Phys. Chem.* **1954**, *58* (2), 110−120.

(27) Ahern, T. J.; Klibanov, A. M. The mechanisms of irreversible enzyme inactivation at 100C. *Science* **1985**, *228* (4705), 1280−1284.

(28) Tomizawa, H.; Yamada, H.; Imoto, T. The Mechanism of Irreversible Inactivation of Lysozyme at pH 4 and 100. degree. C. *Biochemistry* **1994**, *33* (44), 13032−13037.

(29) Tomizawa, H.; Yamada, H.; Tanigawa, K.; Imoto, T. Effects of Additives on Irreversible Inactivation of Lysozyme at Netral pH and 100° C. *J. Biochem.* **1995**, *117* (2), 369−373.

(30) Venkataramani, S.; Truntzer, J.; Coleman, D. R. Thermal stability of high concentration lysozyme across varying pH: A Fourier Transform Infrared study. *J. Pharm. BioAllied Sci.* **2013**, *5* (2), 148.

(31) Ahern, T. J.; Klibanov, A. M. Analysis of processes causing thermal inactivation of enzymes. *Methods Biochem. Anal.* **2006**, 91−128.

(32) Raccosta, S.; Manno, M.; Bulone, D.; Giacomazza, D.; Militello, V.; Martorana, V.; Biagio, P. L. S. Irreversible gelation of thermally unfolded proteins: structural and mechanical properties of lysozyme aggregates. *Eur. Biophys. J.* **2010**, *39* (6), 1007−1017.

(33) Green, R.; Hopkinson, I.; Jones, R. Unfolding and intermolecular association in globular proteins adsorbed at interfaces. *Langmuir* **1999**, *15* (15), 5102−5110.

(34) Steinrauf, L. K.; Dandliker, W. B. A Study of the Reaction of the Disulfide Groups of Bovine Serum Albumin during Heat Denaturation1. *J. Am. Chem. Soc.* **1958**, *80* (15), 3833−3835.
(35) Yang, M.; Dutta, C.; Tiwari, A. Disulfide-bond scrambling promotes amorphous aggregates in lysozyme and bovine serum albumin. *J. Phys. Chem. B* **2015**, *119* (10), 3969−3981.
(36) Yadavalli, N. S.; Borodinov, N.; Choudhury, C. K.; Quiñones-Ruiz, T.; Laradji, A. M.; Tu, S.; Lednev, I. K.; Kuksenok, O.; Luzinov, I.; Minko, S. Thermal Stabilization of Enzymes with Molecular Brushes. *ACS Catal.* **2017**, *7* (12), 8675−8684.
(37) Wang, X.; Yadavalli, N. S.; Laradji, A. M.; Minko, S. J. M. Grafting through Method for Implanting of Lysozyme Enzyme in Molecular Brush for Improved Biocatalytic Activity and Thermal Stability. *Macromolecules* **2018**, *51* (14), 5039−5047.
(38) Yang, C.; Lu, D.; Liu, Z. How PEGylation Enhances the Stability and Potency of Insulin: A Molecular Dynamics Simulation. *Biochemistry* **2011**, *50* (13), 2585−2593.
(39) Murata, H.; Cummings, C. S.; Koepsel, R. R.; Russell, A. J. Polymer-based protein engineering can rationally tune enzyme activity, pH-dependence, and stability. *Biomacromolecules* **2013**, *14* (6), 1919−1926.
(40) Silva, C.; Martins, M.; Jing, S.; Fu, J.; Cavaco-Paulo, A. Practical insights on enzyme stabilization. *Crit. Rev. Biotechnol.* **2018**, *38* (3), 335−350.
(41) DeBenedictis, E. P.; Hamed, E.; Keten, S. Mechanical Reinforcement of Proteins with Polymer Conjugation. *ACS Nano* **2016**, *10* (2), 2259−2267.
(42) Hamley, I. W. PEG−Peptide Conjugates. *Biomacromolecules* **2014**, *15* (5), 1543−1559.
(43) Jain, A.; Ashbaugh, H. S. Helix stabilization of poly (ethylene glycol)−peptide conjugates. *Biomacromolecules* **2011**, *12* (7), 2729−2734.
(44) Shulgin, I. L.; Ruckenstein, E. Preferential hydration and solubility of proteins in aqueous solutions of polyethylene glycol. *Biophys. Chem.* **2006**, *120* (3), 188−198.
(45) Balcão, V. M.; Vila, M. M. D. C. Structural and functional stabilization of protein entities: state-of-the-art. *Adv. Drug Delivery Rev.* **2015**, *93*, 25−41.
(46) Hamed, E.; Xu, T.; Keten, S. Poly(ethylene glycol) Conjugation Stabilizes the Secondary Structure of α-Helices by Reducing Peptide Solvent Accessible Surface Area. *Biomacromolecules* **2013**, *14* (11), 4053−4060.
(47) Zhou, H.-X. Polymer crowders and protein crowders act similarly on protein folding stability. *FEBS Lett.* **2013**, *587* (5), 394−397.
(48) Wang, Y.; Sarkar, M.; Smith, A. E.; Krois, A. S.; Pielak, G. J. Macromolecular Crowding and Protein Stability. *J. Am. Chem. Soc.* **2012**, *134* (40), 16614−16618.
(49) Politou, A.; Temussi, P. A. Revisiting a dogma: the effect of volume exclusion in molecular crowding. *Curr. Opin. Struct. Biol.* **2015**, *30*, 1−6.
(50) Kuznetsova, I. M.; Turoverov, K. K.; Uversky, V. N. What macromolecular crowding can do to a protein. *Int. J. Mol. Sci.* **2014**, *15* (12), 23090−23140.
(51) Ellis, R. J. Macromolecular crowding: an important but neglected aspect of the intracellular environment. *Curr. Opin. Struct. Biol.* **2001**, *11* (1), 114−119.
(52) Senske, M.; Törk, L.; Born, B.; Havenith, M.; Herrmann, C.; Ebbinghaus, S. Protein Stabilization by Macromolecular Crowding through Enthalpy Rather Than Entropy. *J. Am. Chem. Soc.* **2014**, *136* (25), 9036−9041.
(53) Hong, J.; Gierasch, L. M. Macromolecular Crowding Remodels the Energy Landscape of a Protein by Favoring a More Compact Unfolded State. *J. Am. Chem. Soc.* **2010**, *132* (30), 10445−10452.
(54) Makhatadze, G. I.; Privalov, P. L. Protein interactions with urea and guanidinium chloride: a calorimetric study. *J. Mol. Biol.* **1992**, *226* (2), 491−505.
(55) Eggers, D. K.; Valentine, J. S. Molecular confinement influences protein structure and enhances thermal protein stability. *Protein Sci.* **2001**, *10* (2), 250−261.
(56) Morimoto, N.; Yamamoto, M. Design of an LCST−UCST-Like Thermoresponsive Zwitterionic Copolymer. *Langmuir* **2021**, *37* (11), 3261−3269.
(57) Sadhukhan, N.; Muraoka, T.; Ui, M.; Nagatoishi, S.; Tsumoto, K.; Kinbara, K. Protein stabilization by an amphiphilic short monodisperse oligo (ethylene glycol). *Chem. Commun.* **2015**, *51* (40), 8457−8460.
(58) Zhang, D.-L.; Wu, L.-J.; Chen, J.; Liang, Y. Effects of macromolecular crowding on the structural stability of human α-lactalbumin. *Acta Biochim. Biophys. Sin.* **2012**, *44* (8), 703−711.
(59) Sasahara, K.; McPhie, P.; Minton, A. P. Effect of dextran on protein stability and conformation attributed to macromolecular crowding. *J. Mol. Biol.* **2003**, *326* (4), 1227−1237.
(60) Ghosh, S.; Shahid, S.; Raina, N.; Ahmad, F.; Hassan, M. I.; Islam, A. Molecular and macromolecular crowding-induced stabilization of proteins: Effect of dextran and its building block alone and their mixtures on stability and structure of lysozyme. *Int. J. Biol. Macromol.* **2020**, *150*, 1238−1248.
(61) Zielenkiewicz, W.; Swierzewski, R.; Attanasio, F.; Rialdi, G. Thermochemical, volumetric and spectroscopic properties of lysozyme−poly (ethylene) glycol system. *J. Therm. Anal. Calorim.* **2006**, *83* (3), 587−595.
(62) Wu, F.-G.; Jiang, Y.-W.; Chen, Z.; Yu, Z.-W. Folding behaviors of protein (lysozyme) confined in polyelectrolyte complex micelle. *Langmuir* **2016**, *32* (15), 3655−3664.
(63) Chin, J.; Mustafi, D.; Poellmann, M. J.; Lee, R. C. Amphiphilic copolymers reduce aggregation of unfolded lysozyme more effectively than polyethylene glycol. *Phys. Biol.* **2017**, *14* (1), 016003.
(64) Kozer, N.; Kuttner, Y. Y.; Haran, G.; Schreiber, G. Protein-protein association in polymer solutions: From dilute to semidilute to concentrated. *Biophys. J.* **2007**, *92* (6), 2139−2149.
(65) Julius, K.; Weine, J.; Gao, M.; Latarius, J.; Elbers, M.; Paulus, M.; Tolan, M.; Winter, R. Impact of Macromolecular Crowding and Compression on Protein-Protein Interactions and Liquid-Liquid Phase Separation Phenomena. *Macromolecules* **2019**, *52* (4), 1772−1784.
(66) Wu, J.; Zhao, C.; Lin, W. F.; Hu, R. D.; Wang, Q. M.; Chen, H.; Li, L. Y.; Chen, S. F.; Zheng, J. Binding characteristics between polyethylene glycol (PEG) and proteins in aqueous solution. *J. Mater. Chem. B* **2014**, *2* (20), 2983−2992.
(67) Roca, M.; Liu, H.; Messer, B.; Warshel, A. On the relationship between thermal stability and catalytic power of enzymes. *Biochemistry* **2007**, *46* (51), 15076−15088.
(68) Longo, M. A.; Combes, D. Analysis of the thermal deactivation kinetics of alpha-chymotrypsin modified by chemoenzymatic glycosylation. In *Stability and Stabilization of Biocatalysts*; Ballesteros, A., Plou, F. J., Iborra, J. L., Halling, P. J., Eds.; 1998; Vol. *15*, pp 135−140.
(69) Wilcox, X. E.; Ariola, A.; Jackson, J. R.; Slade, K. M. Overlap Concentration and the Effect of Macromolecular Crowding on Citrate Synthase Activity. *Biochemistry* **2020**, *59* (18), 1737−1746.
(70) Mark, A. E.; van Gunsteren, W. F. Simulation of the thermal denaturation of hen egg white lysozyme: trapping the molten globule state. *Biochemistry* **1992**, *31* (34), 7745−8.
(71) Hunenberger, P. H.; Mark, A. E.; van Gunsteren, W. F. Computational approaches to study protein unfolding: hen egg white lysozyme as a case study. *Proteins: Struct., Funct., Genet.* **1995**, *21* (3), 196−213.
(72) Eleftheriou, M.; Germain, R. S.; Royyuru, A. K.; Zhou, R. Thermal denaturing of mutant lysozyme with both the OPLSAA and the CHARMM force fields. *J. Am. Chem. Soc.* **2006**, *128* (41), 13388−95.
(73) Daggett, V.; Levitt, M. Protein Unfolding Pathways Explored Through Molecular Dynamics Simulations. *J. Mol. Biol.* **1993**, *232* (2), 600−619.

https://doi.org/10.1021/acs.langmuir.1c00872
Langmuir 2021, 37, 8474−8485

(74) Tirado-Rives, J.; Jorgensen, W. L. Molecular dynamics simulations of the unfolding of apomyoglobin in water. *Biochemistry* **1993**, *32* (16), 4175−4184.
(75) Mayor, U.; Johnson, C. M.; Daggett, V.; Fersht, A. R. Protein folding and unfolding in microseconds to nanoseconds by experiment and simulation. *Proc. Natl. Acad. Sci. U. S. A.* **2000**, *97* (25), 13518−13522.
(76) Day, R.; Bennion, B. J.; Ham, S.; Daggett, V. Increasing Temperature Accelerates Protein Unfolding Without Changing the Pathway of Unfolding. *J. Mol. Biol.* **2002**, *322* (1), 189−203.
(77) Beck, D. A. C.; Daggett, V. Methods for molecular dynamics simulations of protein folding/unfolding in solution. *Methods* **2004**, *34* (1), 112−120.
(78) Purmonen, M.; Valjakka, J.; Takkinen, K.; Laitinen, T.; Rouvinen, J. Molecular dynamics studies on the thermostability of family 11 xylanases. *Protein Eng., Des. Sel.* **2007**, *20* (11), 551−559.
(79) Meersman, F.; Atilgan, C.; Miles, A. J.; Bader, R.; Shang, W.; Matagne, A.; Wallace, B. A.; Koch, M. H. Consistent picture of the reversible thermal unfolding of hen egg-white lysozyme from experiment and molecular dynamics. *Biophys. J.* **2010**, *99* (7), 2255−63.
(80) Toofanny, R. D.; Daggett, V. Understanding protein unfolding from molecular simulations. *Wiley Interdiscip. Rev.: Comput. Mol. Sci.* **2012**, *2* (3), 405−423.
(81) Du, X.; Sang, P.; Xia, Y.-L.; Li, Y.; Liang, J.; Ai, S.-M.; Ji, X.-L.; Fu, Y.-X.; Liu, S.-Q. Comparative thermal unfolding study of psychrophilic and mesophilic subtilisin-like serine proteases by molecular dynamics simulations. *J. Biomol. Struct. Dyn.* **2017**, *35*, 1500−1517.
(82) Daggett, V.; Levitt, M. A model of the molten globule state from molecular dynamics simulations. *Proc. Natl. Acad. Sci. U. S. A.* **1992**, *89* (11), 5142−5146.
(83) Daggett, V.; Levitt, M. Molecular dynamics simulations of helix denaturation. *J. Mol. Biol.* **1992**, *223* (4), 1121−1138.
(84) Estacio, S. G.; Martiniano, H. F. M. C.; Faisca, P. F. N. Thermal unfolding simulations of NBD1 domain variants reveal structural motifs associated with the impaired folding of F508del-CFTR. *Mol. BioSyst.* **2016**, *12* (9), 2834−2848.
(85) Choudhury, C. K.; Tu, S. D.; Luzinov, I.; Minko, S.; Kuksenok, O. Designing Highly Thermostable Lysozyme-Copolymer Conjugates: Focus on Effect of Polymer Concentration. *Biomacromolecules* **2018**, *19* (4), 1175−1188.
(86) Lee, S.; Tran, A.; Allsopp, M.; Lim, J. B.; Hénin, J.; Klauda, J. B. CHARMM36 United Atom Chain Model for Lipids and Surfactants. *J. Phys. Chem. B* **2014**, *118* (2), 547−556.
(87) Vanommeslaeghe, K.; MacKerell, A. D. Automation of the CHARMM General Force Field (CGenFF) I: Bond Perception and Atom Typing. *J. Chem. Inf. Model.* **2012**, *52* (12), 3144−3154.
(88) Mahoney, M. W.; Jorgensen, W. L. A five-site model for liquid water and the reproduction of the density anomaly by rigid, nonpolarizable potential functions. *J. Chem. Phys.* **2000**, *112* (20), 8910−8922.
(89) Abraham, M. J.; Murtola, T.; Schulz, R.; Páll, S.; Smith, J. C.; Hess, B.; Lindahl, E. GROMACS: High performance molecular simulations through multi-level parallelism from laptops to supercomputers. *SoftwareX* **2015**, *1−2*, 19−25.
(90) Van der Spoel, D.; Lindahl, E.; Hess, B.; Groenhof, G.; Mark, A. E.; Berendsen, H. J. C. GROMACS: Fast, flexible, and free. *J. Comput. Chem.* **2005**, *26* (16), 1701−1718.
(91) Ilavsky, J.; Jemian, P. R. Irena: tool suite for modeling and analysis of small-angle scattering. *J. Appl. Crystallogr.* **2009**, *42* (2), 347−353.
(92) Micsonai, A.; Wien, F.; Kernya, L.; Lee, Y.-H.; Goto, Y.; Réfrégiers, M.; Kardos, J. Accurate secondary structure prediction and fold recognition for circular dichroism spectroscopy. *Proc. Natl. Acad. Sci. U. S. A.* **2015**, *112* (24), E3095−E3103.
(93) Micsonai, A.; Wien, F.; Bulyáki, É.; Kun, J.; Moussong, É.; Lee, Y.-H.; Goto, Y.; Réfrégiers, M.; Kardos, J. BeStSel: a web server for accurate protein secondary structure prediction and fold recognition from the circular dichroism spectra. *Nucleic Acids Res.* **2018**, *46* (W1), W315−W322.
(94) Strazdaite, S.; Navakauskas, E.; Kirschner, J.; Sneideris, T.; Niaura, G. Structure Determination of Hen Egg-White Lysozyme Aggregates Adsorbed to Lipid/Water and Air/Water Interfaces. *Langmuir* **2020**, *36* (17), 4766−4775.
(95) Kaur, M.; Singh, G.; Kaur, A.; Sharma, P. K.; Kang, T. S. Thermally Stable Ionic Liquid-Based Microemulsions for High-Temperature Stabilization of Lysozyme at Nanointerfaces. *Langmuir* **2019**, *35* (11), 4085−4093.
(96) Saeki, S.; Kuwahara, N.; Nakata, M.; Kaneko, M. Upper and lower critical solution temperatures in poly (ethylene glycol) solutions. *Polymer* **1976**, *17* (8), 685−689.
(97) Kameta, N.; Matsuzawa, T.; Yaoi, K.; Masuda, M. Short polyethylene glycol chains densely bound to soft nanotube channels for inhibition of protein aggregation. *RSC Adv.* **2016**, *6* (43), 36744−36750.
(98) Smith, G. D.; Bedrov, D. Roles of Enthalpy, Entropy, and Hydrogen Bonding in the Lower Critical Solution Temperature Behavior of Poly(ethylene oxide)/Water Solutions. *J. Phys. Chem. B* **2003**, *107* (14), 3095−3097.
(99) Chudoba, R.; Heyda, J.; Dzubiella, J. Temperature-Dependent Implicit-Solvent Model of Polyethylene Glycol in Aqueous Solution. *J. Chem. Theory Comput.* **2017**, *13* (12), 6317−6327.
(100) Kjellander, R.; Florin, E. Water structure and changes in thermal stability of the system poly(ethylene oxide)−water. *J. Chem. Soc., Faraday Trans. 1* **1981**, *77* (9), 2053−2077.
(101) Van Gunsteren, W. F.; Hünenberger, P. H.; Kovacs, H.; Mark, A. E.; Schiffer, C. A. Investigation of protein unfolding and stability by computer simulation. *Philos. Trans. R. Soc., B* **1995**, *348* (1323), 49−59.
(102) Keefe, A. J.; Jiang, S. Poly(zwitterionic)protein conjugates offer increased stability without sacrificing binding affinity or bioactivity. *Nat. Chem.* **2012**, *4* (1), 59−63.
(103) Klibanov, A. M. Improving enzymes by using them in organic solvents. *Nature* **2001**, *409* (6817), 241−246.

https://doi.org/10.1021/acs.langmuir.1c00872
Langmuir 2021, 37, 8474−8485